2013

Optical and Mechanical Characterization of Dental Hard Tissue

MANDURAH, Mona

Mohammad M.

Doctoral of Philosophy Thesis

Optical and Mechanical Characterization of Dental Hard Tissue

Presented by

Mona Mohammad M. Mandurah

To

Cariology and Operative Dentistry,
Oral Health Sciences Department, Faculty of Dentistry,
Graduate School of Medical and Dental Sciences

in partial fulfillment of the requirements
for the degree of
Doctor of Philosophy
in Dental Science

Promoter: Prof. Junji TAGAMI
Advisors: Drs. Alireza Sadr & Yasushi Shimada

Tokyo Medical and Dental University
Tokyo, Japan
August 2013

Promoter: Prof. Junji TAGAMI

Author: Dr. Mona MANDURAH

Cariology and Operative Dentistry

Optical and Mechanical Characterization of Dental Hard Tissue

Abstract

[Background and Objective]: Although the teeth are considered the hardest part in human body, they are subjected to many changes including caries formation, demineralization, cracks formation and attrition with aging. Detecting early stages of enamel demineralization and remineralization was our concerns. Changes of superficial area under attrited teeth were another concern. Recently, with the development of technology in the medical and dental fields, it was believed that assessment of minor changes in dental tissues is not impossible with the present of optical coherence tomography. OCT is a non-invasive, non-destructive method that has been addressed recently as a substitution method to the invasive method used laboratory and clinically. The aim of this study was to monitor remineralization of enamel subsurface lesion by OCT and to characterize the sclerotic dentin under attrition teeth.

[Materials and Methods]: Both human and bovine teeth were used in this study. Attrited human teeth were used for sclerotic dentin assessment and bovine teeth were used for monitoring remineralization enamel subsurface lesion. Serial cross-sectional images were taken be swept source optical coherence tomography (SS-OC) for sclerotic dentin and monitoring remineralization of enamel subsurface lesion. Then cross-sectioned specimen were obtained from the samples, polished well and subjected to nanoindentation for hardness test. Signal analysis of obtained images from OCT was done.

[Results]: Generally OCT signals of enamel appeared steadier than dentin due to transmitting of light through enamel prisms is much easier than through dentinal tubules. Increased SS-OCT signals in the dental hard tissue indicate changes in the mineral content. High signal intensity from the surface indicates mineral loss, with remineralization, the signal slope decrease.

[Conclusion]: SS-OCT imaging technology is a promising modality that can be used clinically as a non-invasive technique to detect any change in dental hard tissue.

DEDICATION

DEDICATION

This work is dedicated to the great source of inspiration and motivation, my father Dr. Mohammad MANDURAH, mother Najwa MANDURAH, my brothers and sisters.

Also, I dedicate this work to my friends for their uncountable support and assistance.

Lastly and most importantly, I dedicate this work to my darling husband Dr. Turki BAKHSH and beloved daughter Lamar and son Abdullah, for their never-ending love, understanding and support.

ACKNOWLEDGMENTS

ACKNOWLEDGMENTS

I would like to express my heartfelt gratitude and appreciation to the Chairman of Cariology and Operative Dentistry, Oral Health Science Department, my mentor **Prof. Junji TAGAMI**, who always inspires me not only to get perceptions into science, but also to gain knowledge outside science. I am deeply grateful to Dr. Y. SHIMADA, Dr. S. NAKASHIMA, Dr. M. OTSUKI, Dr. Y. KITASAKO, Dr. T. NIKAIDO, Dr. M. NAKAJIMA, Dr. T. YOSHIKAWA, Dr. G. INOUE, Dr. E. CHO, Dr. K. HOSAKA, Dr. T. TAKAGAKI, Dr. H. HAMBA Dr. N. SEKI and Dr. R. TAKAHASHI for their encouragement and extensive logistical support.

I would also like to express my sincere appreciation to Dr. Patricia MAKISHI, Dr. Yuko NATSUME, Dr. Ilnaz HARIRI Dr. Hamid NURROHMAN, Dr. Amir NAZARI, Dr. Taweesak PRASANSUTTIPORN, Dr. Suppason THITTHAWEERAT, Dr. Gerardo MENDEZ, Dr. Sofiqul ISLAM, Dr. Hisaichi NAKAGAWA, Dr. Ena LODHA, Dr. Aidil AKMAL, Dr. Mohannad NASSAR, Dr. Ornicha THANATVARAKORN, Dr. Alaa TURKISTANI, Dr. Sahar KHUNKAR, Dr. Ehab AL-SAYED, Dr. Baba BISTA, Dr. Maja ROMERO, Dr. Patricia MAJKUT and my colleagues in TMDU student Chapter, and all the people in this department, for their friendship and invaluable involvement in scientific discussions and generous support.

I would like to address a special acknowledgment for my Advisor **Dr. Alireza SADR**, Chaperon in Global–COE at Tokyo Medical and Dental University, for his patience and indefinite guidance in helping me to get into the academic research, for his unconditional support, and for providing me the opportunity to conduct research in different field of dentistry under his constructive comments. His expertise, and help in every step of my project. His creative, guidance and endless dedication gave me great motivation to think differently. His encouragement and enthusiasm made my graduate training at Tokyo Medical and Dental University a memorable and meaningful experience. I learned a lot from him and he was one of the most influencing people in my life. I will never be able to express my gratitude to him and show how much I respect and appreciate him.

Finally, to all those people who I did not mention their names, but in one way or another have been an inspiration to me and provided greatest assistance, I sincerely thank you all.

PREFACE

PREFACE

This thesis is based on the original research works by the author, to which the following articles refer.

Article 1. **Mandurah MM,** Sadr A, Shimada Y, Kitasako Y, Nakashima S, Bakhsh TA, Tagami J, Sumi Y. "Monitoring remineralization of enamel subsurface lesion by optical coherence tomography" J. Biomed. Opt. 18(4) 2013

Article 2. **Mandurah MM,** Sadr A, Bakhsh TA, Shimada Y, Tagami J, Sumi Y. "Characterization of transparent dentin of attrited teeth using optical coherence tomography and nanoindentation" (Under consideration for publication)

TABLE OF CONTENTS

CONTENTS

CHAPTER 3:

CHAPTER 4:

LIST OF FIGURES

LIST OF FIGURES

Figure

CHAPTER 1

1. BACKGROUND AND LITRATURE REVIEW

Dental hard tissue, consisting of enamel and dentin are the most important parts of teeth. Enamel is the outer surface layer that consists of inorganic minerals while the dentin consists mainly of collagen (1). Knowing the anatomy and optical properties of sound enamel and dentin are considered from the basics in dental field. In the past decades, many methods were used to detect dental caries lesion and odontogenic diseases, X-ray and CT- scan are of the most well-known machines. Although the usage of these methods has been widespread in the medical field, the biohazards of these methods are the most concern. The x-ray waves considered harmful to the living tissue in a long term (2). Recently with the development of technologies, small enamel and dentin lesion can be easily detected without the use of invasive methods that depends on the electromagnetic field, which can harm the dental tissue and the human cells. Beside the visual examination of the caries, other diagnostic methods based on light-induced or laser-stimulated fluorescence have been developed (3-5). Nevertheless, these systems do not provide cross-sectional images of the dental structure and their effectiveness to track the minimal changes in enamel subsurface lesion has been moderate. Therefore, the development of a user-friendly technology to assist real-time characterization of early lesions is among research priorities recommended by expert work groups (6).

Optical coherence tomography (OCT) is a non-invasive, cross-sectional imaging system that can visualize the internal structures non-destructively (7). OCT was developed on the concept of low-coherence interferometry where the light is projected over a sample, and the backscattered signal intensity from the scattering medium reveals depth resolved information

about scattering and reflection of the light in the sample. It performs cross-sectional images generated by performing multiple axial measurements of echo time delay (axial scans or A-scans) and scanning the incident optical beam transversely. This generates a two-dimensional data set, which represents the optical backscattering in a cross-sectional plane through the tissue. Images or B-scans can be displayed in a false color or grey scale to visualize tissue changes. The conventional OCT imaging system was based on the principles of time-domain OCT (TD-OCT), where a mirror mechanically scans a distance at the reference arm to enable resolving of the depth information. More recently spectral-domain OCT systems have been developed, in which the mechanical scanning at the reference mirror has been eliminated and the images are obtained in a shorter time (8). Simplification of this system by encoding the spectral components (wavenumber) in time generated the swept-source OCT (SS-OCT). In this technology, the laser source sweeps near-infrared wavelength within milliseconds scan delays at kilohertz rates in order to achieve real-time imaging. SS-OCT is the latest implementation of imaging technology with a promising prospect as a chair-side diagnostic modality in dentistry, due to its enhanced 2D and 3D scanning speed and image resolution. (Fig.1) This modality has been validated to score carious lesion extent and detect cracks and dental restoration defects (9-11).

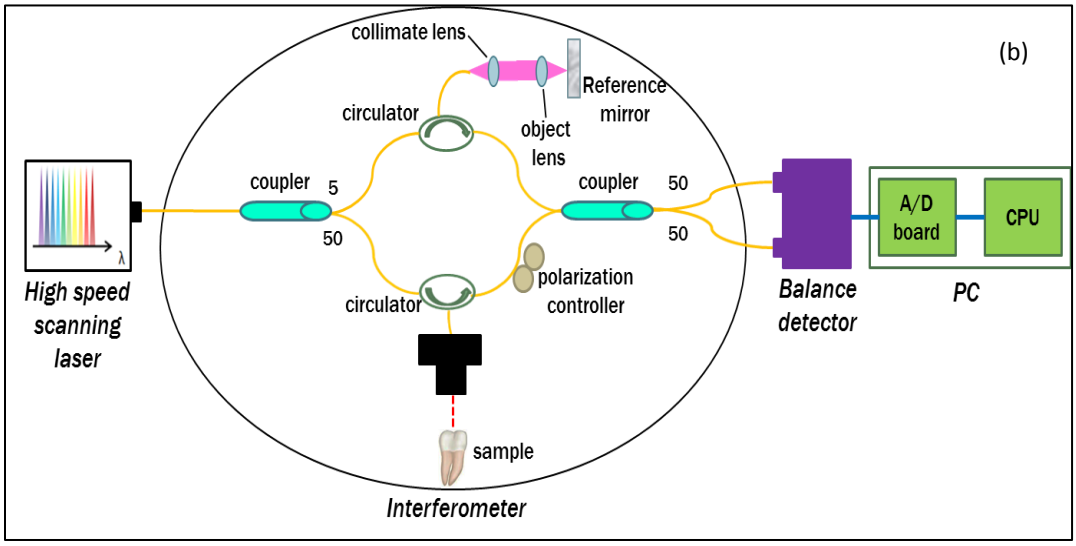

Figure-1: (a) The SS-OCT system (OCT-2000, Santec, Komaki, Japan), (b) Each scan of wavelengths produces an interference pattern signal by the reflections at different depths. Depth dependent reflection profiles are calculated by Fourier transform of the interferogram. Repeating this A-scan at different locations produces a two dimensional cross section.

OCT has been widely used in assessment of demineralization based on two main principles; increased light scattering in the porous demineralized tissue, and depolarization of the incident light by the demineralized tissue. The latter necessitates a polarization-sensitive OCT (PS-OCT)

or cross-polarization OCT setup, (12-14) but the former phenomenon can be observed as increased signal intensity by both conventional and polarized-sensitive OCT systems. Image analysis techniques in correlative OCT studies have been mainly based on the increased signal intensity values to quantify parameters such as depth (as a cut-off point) and mineral loss (dB) values integrated over depth) in demineralized lesions;(15) however, there are fewer studies on the assessment of remineralization by conventional OCT or sclerotic dentin.

In this thesis two studies based on OCT, the first one is to monitor the remineralization of early enamel lesion, and the other one to detect sclerotic dentin of attrited teeth.

CHAPTER 2: MONITORING REMINERALIZATION OF ENAMEL SUBSURFACE LESION BY OPTICAL COHERENCE TOMOGRAPHY

CHAPTER 2

MONITORING REMINERALIZATION OF ENAMEL SUBSURFACE LESION BY OPTICAL COHERENCE TOMOGRAPHY

2.1. INTRODUCTION AND OBJECTIVES

Dental caries is a multi-factorial disease process that results in localized dissolution and destruction of the calcified dental tissues. An incipient lesion or subsurface lesion is a type of caries that has an intact enamel surface with no cavitation (16, 17). Developing of an enamel lesion without breakdown of the outer surface is more common in case of early lesions. The surface layer covering the lesion is usually a mineral rich area with less dissolution susceptibility, which is unlike the subsurface area where the dissolution takes place and has less mineral content (16). Once the lesion reaches the dentin, it will spread eventually causing progression of the lesion with intact enamel, at which stage a surgical intervention to remove the caries is inevitable (18). On the other hand, the demineralization process can be reversed, especially at early stages, in the presence of bioavailable calcium and phosphate ions in the environment. It is believed that remineralization would also be accelerated or enhanced by the effect of fluoride (19). For instance, the addition of calcium and phosphate in the form of phosphoryl oligosaccharide of calcium (POs-Ca) or that with fluoride (POs-Ca+F) to a chewing gum (Ezaki Glico, Osaka, Japan) enhanced enamel remineralization of subsurface enamel lesions in a clinical study (20, 21)

Early detection of these incipient caries followed by objective monitoring in the course efforts to arrest or remineralize them is critical concerns in the modern dentistry. Visual inspection is one of the most common diagnostic methods in lesion assessment. Although the International Caries Detection and Assessment System (now ICDAS-II), based on visual examination, has been introduced as a novel system to diagnose dental caries, (22) however the subjectivity of this method could affect its usage. Conventional radiography is suitable for cavitated lesions but not early incipient lesions due to low resolution and superimposition of structures that could impede the correct diagnosis of the exact lesion (23). Other diagnostic methods based on light-induced or laser-stimulated fluorescence and electric conductivity have been developed (3, 5, 24). Nevertheless, these systems do not provide cross-sectional images of the dental structure and their effectiveness to track the minimal changes in enamel subsurface lesion has been moderate. Therefore, the development of a user-friendly technology to assist real-time characterization of early lesions is among research priorities recommended by expert work groups (6).

Optical coherence tomography (OCT) is a non-invasive, cross-sectional imaging system that can visualize the internal structures non-destructively (7). OCT was developed on the concept of low-coherence interferometry where the light is projected over a sample, and the backscattered signal intensity from the scattering medium reveals depth resolved information about scattering and reflection of the light in the sample. It performs cross-sectional images generated by performing multiple axial measurements of echo time delay (axial scans or A-scans) and scanning the incident optical beam transversely. This generates a two-dimensional data set, which represents the optical backscattering in a cross-sectional plane through the tissue. Images or B-scans can be displayed in a false color or grey scale to visualize tissue changes. The

conventional OCT imaging system was based on the principles of time-domain OCT (TD-OCT), where a mirror mechanically scans a distance at the reference arm to enable resolving of the depth information. More recently spectral-domain OCT systems have been developed, in which the mechanical scanning at the reference mirror has been eliminated and the images are obtained in a shorter time (8). Simplification of this system by encoding the spectral components (wavenumber) in time generated the swept-source OCT (SS-OCT). In this technology, the laser source sweeps near-infrared wavelength within milliseconds scan delays at kilohertz rates in order to achieve real-time imaging. SS-OCT is the latest implementation of imaging technology with a promising prospect as a chair-side diagnostic modality in dentistry, due to its enhanced 2D and 3D scanning speed and image resolution. This modality has been validated to score carious lesion extent and detect cracks and dental restoration defects (11, 25-27).

OCT has been widely used in assessment of demineralization based on two main principles; increased light scattering in the porous demineralized tissue, and depolarization of the incident light by the demineralized tissue. The latter necessitates a polarization-sensitive OCT (PS-OCT) or cross-polarization OCT setup, (14, 28, 29) but the former phenomenon can be observed as increased signal intensity by both conventional and polarized-sensitive OCT systems. Image analysis techniques in correlative OCT studies have been mainly based on the increased signal intensity values to quantify parameters such as depth (as a cut-off point) and mineral loss (dB values integrated over depth) in demineralized lesions;(15) however, there are fewer studies on the assessment of remineralization by conventional OCT.

Quantitative measurement of other optical properties that are based on light propagation in tissue may potentially provide a repeatable means of the tissue characterization. Among those

properties, the attenuation coefficient has shown promising results in discriminating between healthy and diseased states of various tissues including the epithelial tissues, arteries, skin, and lymph nodes (30, 31). This parameter was noted in relation to enamel demineralization and remineralization,(32, 33) however, few studies have validated the parameter at the 1300 nm OCT wavelength range against physical properties of enamel such as hardness.

The aim of this study was to evaluate the optical changes and attenuation coefficient in the remineralized enamel subsurface lesion by POs-Ca with or without fluoride, and to correlate these findings with their mechanical hardness using nanoindentation test. Two null hypotheses were established in this study; 1: attenuation coefficient derived from OCT signal did not depend on enamel mineral condition. 2: there was no correlation between the OCT parameter and nanoindentation hardness.

2.2. MATERIALS AND METHODS

2.2.1 PREPARATION OF THE SAMPLES

Fresh bovine incisors were obtained from a local slaughter house (Yokohama, Japan). After cleaning the bovine teeth from debris and soft tissue, enamel blocks (7 mm × 10 mm × 2 mm) (width × length × depth) were cut from the incisors using a low speed diamond saw (Isomet; Buehler, Lake Bluff, IL, USA) under running water, and embedded in acrylic resin (Unifast Trad; GC, Tokyo, Japan). The outer enamel surface was polished to a mirror finish using wet polishing papers (800, 1000, 1200, 1500 and 2000 grit lapping papers; 3M, St. Paul, MN, USA). Three areas, namely sound (SND), demineralized (DEM), and remineralized (REM) were assigned on the polished enamel surface of each block as follows: First, one third of the surface on each block was covered with a nail varnish (nail POP; Chamon, Kyonggi, South Korea); which served as the SND portion. Subsurface lesion were then formed on the remaining surface using the two–layer demineralization method with 8% methylcellulose gel (Methocel MC, Fluka, Everett, WA, USA) and 0.1 M lactate buffer (pH 4.6) at 37°C for 14 days (34). The ratio of gel to lactate buffer was 3:5, respectively. After demineralization, the blocks were sterilized by ethylene oxide gas sterilizer (Steri-Gas; 3M, St. Paul, MN, USA). The middle-third of the surface was kept as DEM area, and the remaining third of enamel surface, which was cut away by low speed saw, served as REM area as described below.

2.2.2 IMMERSION IN REMINERALIZING SOLUTION

Eight demineralized specimens (n=8) were immersed in 10 ml of one of the three differently prepared solutions for up to 14 days; deionized water as control group (H_2O), POs-Ca remineralizing solution group which contains 100 mM KCl, 3.6 mM KH_2PO_4, 1.5 mM $CaCl_2$, 20

mM HEPES, plus 0.36% of POs-Ca (pH=6.5), and POs-Ca+F remineralizing solution group that was similar in composition to POs-Ca group, but with the addition of 1 ppm of fluoride extracted from green tea (POs-Ca+F). The specimens were stored in incubator at 37°C and the pH of the solutions was monitored and refreshed daily.

2.2.3 OCT SYSTEM

The SS-OCT system (OCT-2000, Santec, Komaki, Japan) incorporates a high-speed frequency swept external cavity laser, and the wavelength ranged from 1260 to 1360 nm (centered at 1310 nm) at a 20-kHz sweep rate. Backscattered light from the subject is coupled back to the OCT system, in which the interference signal is digitized in time scale, and then analyzed in the Fourier domain to reveal the depth information of the subject. The axial and lateral resolutions of the system in air were 11 and 17 μm, respectively. The system acquired the image data (B-scan) in 0.3 s, including the processing time. The imaging range in this study was 5 mm (width) by 6.6 mm (height), forming a 2000 × 1019 pixel image. The sensitivity of this system and the shot-noise limited sensitivity were 106 and 119 dB, respectively.

2.2.4 OCT IMAGING OF THE SPECIMENS

The hand-held scanning probe connected to the OCT system was set at 5 cm distance from the specimen surface, with the scanning beam oriented about 90 degree to the surface. A custom-made jig was mounted on a micrometer stage to keep each specimen surface parallel to the probe plane.

For each specimen, the cross-sectional images were acquired from SND and DEM areas as well as REM area after 4, 7 and 14 day of remineralization, at the center of the window. The

specimens were removed from the solutions, cleaned with ultrasonic to remove any precipitants on the surface and washed by distilled water, and then OCT images were scanned in controlled hydrated condition after blot drying of the surface with no visible water droplets (35). In order to ensure the repeatability of the OCT scan during remineralization, the specimens were placed at the same orientation as accurately as possible every time, and the B-scan was performed along a line between two points marked by a marker pen on the specimen surface.

2.2.5 OCT IMAGE ANALYSIS

For image analysis, a custom code in the image analysis software (ImageJ version 1.45S; Wayne Rasband, NIH, Bethesda, Maryland) was used to read the raw data of the OCT. The obtained OCT image was rotated to compensate for the tilting during scan and reach a horizontal surface. A noise reducing median filter (size 2) was applied to the data. A region of interest (ROI, width 200 μm × optical depth 400 μm) from the surface of enamel to deeper levels was selected and converted to signal intensity depth profile.

The OCT-attenuation coefficient (μ_t) was calculated on each average signal intensity profile based on the exponential decay of irradiance from the surface of the specimen using the equation derived from Beer-Lambert law, in the following function (36).

$$I(z) \propto e^{-2\mu_t z} \quad \text{Eq. (1)}$$

Where I is the reflectivity signal intensity in (dB) and z is the depth variable in mm. μ_t was calculated using linear least-squares regression to fit the natural log of average OCT profiles obtained from the ROI.

$$\mu_t \propto -\frac{\ln I(z)}{2z} \quad \text{Eq. (2)}$$

2.2.6 NANOHARDNESS TEST

Sections from the SND, DEM and 14 day REM areas used for OCT were then embedded in epoxy resin (EpoxiCure; Buehler, Lake Bluff, IL, USA). In order to produce smooth cross-sectional surfaces suitable for nanoindentation test, each sample was sequentially trimmed and polished by silicon-carbide papers in an ascending order starting from #600 and up to #2000, followed by diamond slurries with particle sizes of ranging from 6 μm to 0.25 μm by using an automatic lapping machine (Maruto, Tokyo, Japan). The nanohardness profiles of the DEM and REM areas were measured with a nanoindentation device (ENT-1100a; Elionix, Tokyo, Japan) down to 220 μm in depth. On each area across the polished cross-section, a minimum of 400 indentations were performed along 40 rows each with 10 points, with a spacing of 10 μm between each 2 neighboring points; the first 200 indentation points were programmed on 20 lines with 1 μm distance between each 2 adjacent lines (first 20 μm) in the axial direction. The first row was within resin approximately right above the visible enamel border. The next 200 points started 10 μm below the last row of indentations with 10 μm spacing in axial direction (final depth of 220 μm). For all indentations, the maximum load was 2 mN with loading rate of 0.2 mN/sec and using a Berkovich diamond tip. The nanoindentation was performed on three samples in each group. In sum, over 10,000 indentations were performed in this study. To calculate Martens hardness (H) in MPa, the load was divided over the projected area under maximum load which would include both elastic and plastic deformation.

$$H = \frac{Force}{Contact\ area} \quad \text{Eq. (3)}$$

In addition to the hardness profile for each area, integrated nanohardness (INH) values were calculated for the whole lesion, as the area under the hardness-depth curve up to the average lesion depth (140 μm).

2.2.7 STATISTICAL ANALYSIS

Pearson's correlation was used to examine the relationship between μ_t and INH for each specimen including SND, REM and DEM areas. Kolmogorov Smirnoff tests were used to determine normal distribution of the data and select proper analyses. Repeated measures ANOVA was used to compare μ_t among groups with time series as the factor. In order to compare μ_t at different times within each remineralizing solution, one-way ANOVA with Tukey's post-hoc test was used. Similarly, INH values were analyzed by one-way ANOVA with Tukey's post-hoc test between the groups. All statistical analyses were performed with 95% level of confidence with Statistical Package for Medical Science (SPSS Ver.11 for Windows, SPSS, Chicago, IL, USA) ($\alpha = 0.05$).

2.3 RESULTS

OCT images of SND, DEM and REM enamel in each group are presented in Fig. 1. There was a conspicuous prominence of the enamel lesion shown in the OCT image of DEM area, with a high reflectivity from the lesion and a sudden drop of the reflectivity just beneath the lesion, which revealed a lesion boundary. The optical lesion depth (from the surface to the boundary) was 214 ± 13 μm. The real depth can be calculated by dividing the optical depth over the approximate refractive index of enamel (1.6) which was equal to 134.1 ± 8 μm. With remineralization in both POs-Ca groups, the intensity of the optical boundary declined and visual

changes were observed in the OCT image. Figure 2(a) represents OCT signal intensity profiles obtained from the ROI, with the fitted lines to calculate μ_t in Fig. 2(b).

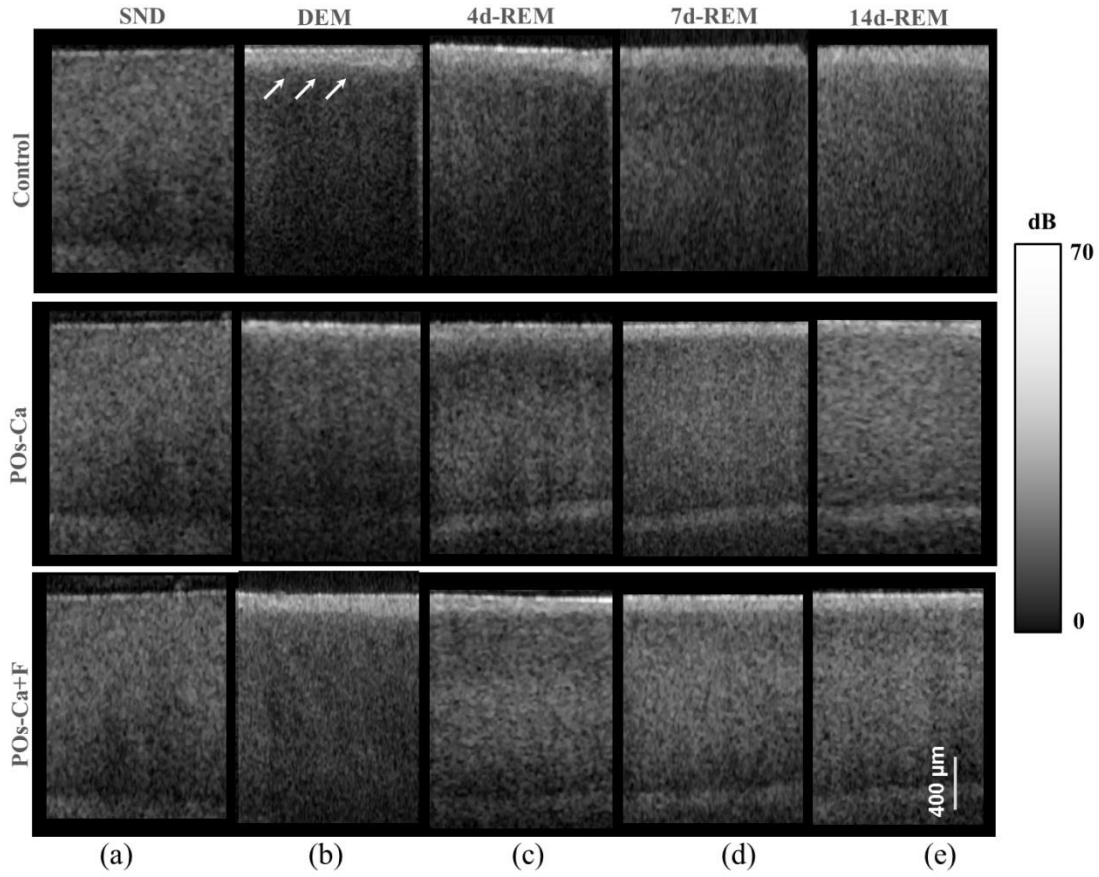

Figure-2: B-scan images of SS-OCT of Control, POs-Ca and POs-Ca+F groups, arrows indicate the lesion boundary and the vertical scale bar represents 400 µm optical axial distance (a) Sound enamel, (b) DEM, (c) after 4-day remineralization, (d) after 7-day remineralization, and (e) after 14-day remineralization.

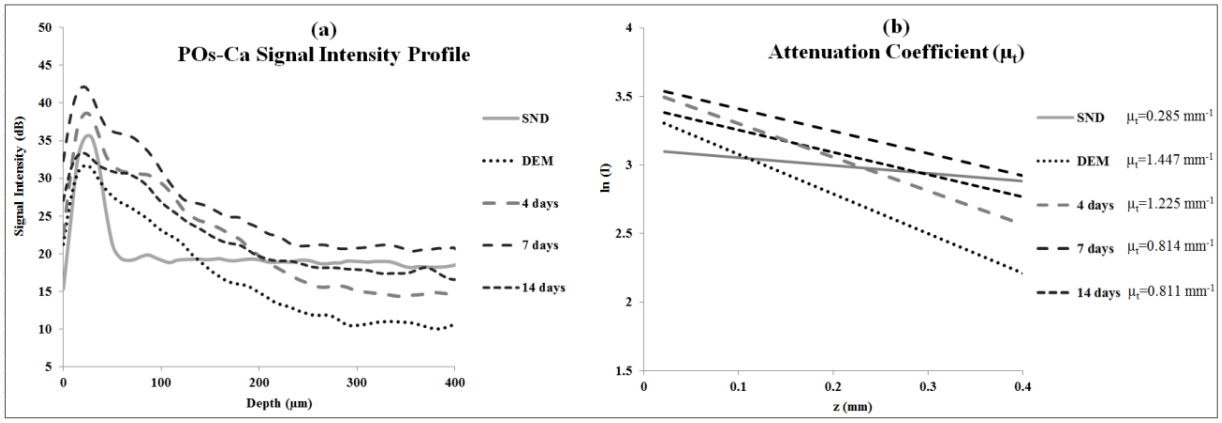

Figure-3: (a) Signal intensity profile of POs-Ca showing sound, DEM, 4 days, 7 days and 14 days remineralization. Remieneralization resulted in higher signal levels from deeper areas. (b) An OCT attenuation coefficient (µt) was calculated using linear least-squares regression to fit the natural log of average OCT profiles obtained from the ROI. The sound enamel has the lowest µt attenuation coefficient while the DEM has the highest. With remineralization, a decrease in the parameter values was evident. Note that the Beer-Lambert law takes a depth factor of 2.

Nanoindentation confirmed that both POs-Ca+F and POs-Ca resulted in remineralization of the whole lesion. Figure 3(a) demonstrates a stereo microscopic image of a representative sample after nanoindentation. The mean hardness profiles of all groups are shown in Fig. 3(b). As confirmed by INH, REM areas showed remarkable improvement compared to the corresponding DEM areas, except for the control group. While the hardness of surface layer (superficial 10 µm) appeared to be higher in POs-Ca+F group, there was no significant difference in INH between POs-Ca+F (438 ± 13 GPa▪µm) and POs-Ca (442 ± 17 GPa▪µm) ($p>0.05$), [Fig. 3(c)]. None of the treatments resulted in recovering to the INH of SND enamel

(574 ± 3 GPa▪µm) ($p<0.05$).

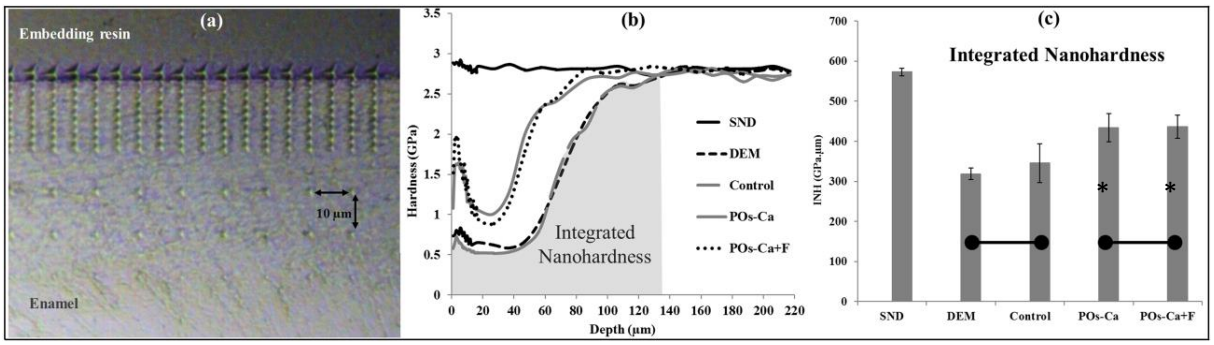

Figure-4: (a) Optical microscopic image of polished enamel surface after nanoindentation. (b) Mean hardness profile for SND, DEM, Control, POs-Ca and POs-Ca+F areas. (c) A bar graph showing INH of all groups; asterisk (*) shows significant difference with DEM ($p<0.05$). Horizontal bar indicates no significant difference among time subgroups ($p>0.05$).

There was a good correlation between the optical and mechanical parameters; μ_t and INH. With remineralization μ_t decreased and INH increased (Pearson's correlation $p<0.001$, $r=-0.97$, 95% CI for r = -0.99 to -0.93). A linear regression was established between the two parameters ($R^2=0.94$, Fig. 4), validating the μ_t parameter.

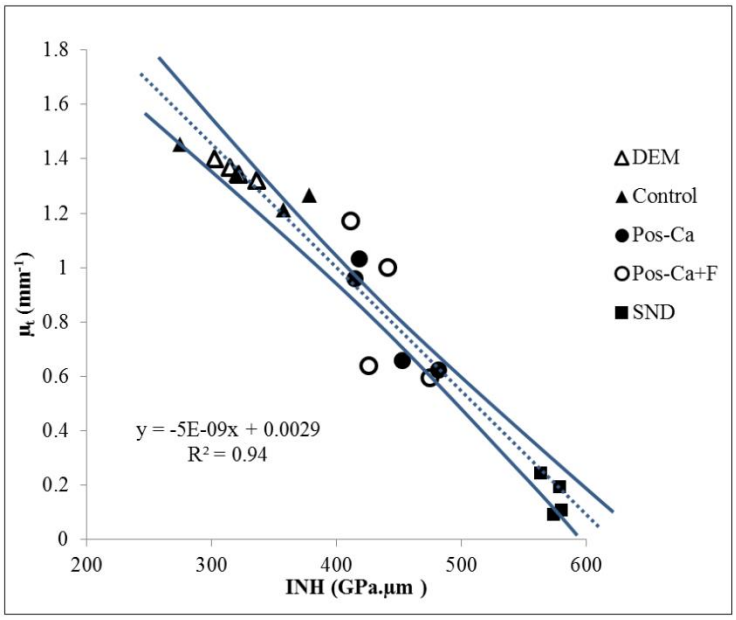

Figure-5: μ_t and INH correlation (P<0.001, r=-0.97 95% CI: -0.99 to -0.93), the best regression was established with a linear fit (R2=0.94). 95% CIs of the fit line are displayed.

The average μ_t data of all groups are summarized in a chart (Fig. 5). Repeated measures ANOVA showed that the within subject factor (remineralization time) significantly affected μ_t ($F=14.9$, $p<0.001$). Similarly, the between-subject factor (remineralization solution) and the interaction of the factors were significant ($p<0.001$). The μ_t of SND area showed the smallest reading (range 0.08 to 0.29 mm^{-1}) which meant that the fitting line had the lowest slope; on the other hand, DEM areas showed the highest μ_t values which ranged between 1.34-1.47 mm^{-1}; this indicated rapid loss of signals in deeper areas. With remineralization, μ_t values significantly recovered in POs-Ca and PO-Ca+F groups ($p<0.05$) reaching up to mean values of 0.81 and 0.85 mm^{-1} respectively; meanwhile, there was no noticeable change in the control group ($p>0.05$). POs-Ca+F showed a rapid and significant drop in μ_t at day 4 ($p<0.05$), but no further decrease took place after that. On the other hand, POs-Ca group showed gradual decrease in the attenuation coefficient up to 7 days of remineralization ($p<0.05$), but no significant difference was detected after that. μ_t values of PO-Ca+F and POs-Ca were close to each other at the end of 14-day remineralization.

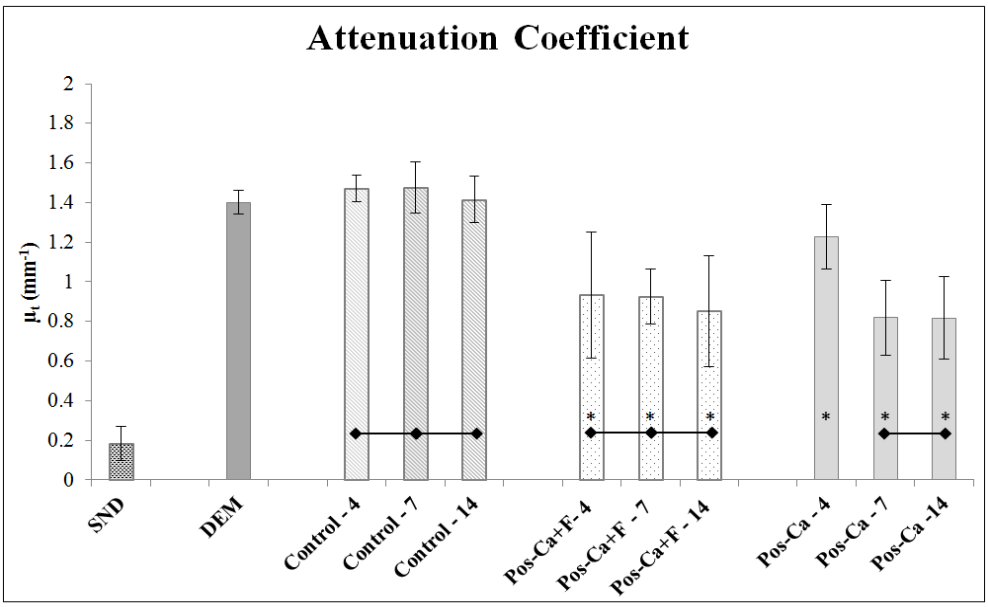

Figure-6: The bar graph shows μt of different groups through remineralization days. Asterisk (*) indicates significant difference with DEM ($p<0.05$). Horizontal bar indicates no significant difference among time subgroups ($p>0.05$)

2.4 DISCUSSION

In this study, we examined the capability of OCT to detect changes induced by de/remineralization in enamel subsurface lesion. The B-scan images obtained from both treatment groups displayed a decrease in the reflectivity of the lesion body with a decreased contrast at the lesion boundary. In a previous study, it was shown that OCT had the potential for quantitative estimation of lesion depth and mineral loss in demineralized dentin lesion, which revealed a definite boundary suggesting the lesion front (15). The appearance of enamel lesion boundary was also shown in another study (35). In fact, this appearance has been the basis for scoring the extent of natural caries using OCT (26, 37). These studies suggest that backscatter

signal intensity increases with demineralization due to scattering at the numerous micro interfaces created in the hard tissue by the dissolution process of mineral (15, 37). Oppositely, it was expected that the signal intensity would decrease when porosities were filled by mineral aggregation during remineralization. Nevertheless, in the current study, some remineralized samples showed slight change or increase in the signal intensity from the surface zone [Fig. 2(a)], which made it difficult to perform objective comparisons using the integrated or mean intensity parameters commonly known for PS-OCT (13, 38).

Attenuation can be regarded as another parameter for analysis of OCT backscatter signal. Sound enamel strongly attenuates light in the visible range, but the magnitude of scattering at higher wavelengths is lower than in the visible range. OCT imaging of early lesions at 850 nm showed that signal patterns and attenuation were different between sound enamel and early enamel lesion.(32, 39). It is noteworthy that in the near infra-red region around 1300 nm wavelength sound enamel becomes highly transparent (40, 41). while at smaller wavelength (e.g. 850 nm) sound enamel attenuates the signal and there is an effective imaging depth of around 100 μm (39). A previous study suggested that at this wavelength, the OCT signal slope of human enamel surface at a few hundred micrometers from the surface did not greatly depend on the prismatic orientation, and was much smaller than that of dentin (42). confirming that the magnitude of light scattering in sound enamel is prominently lesser than dentin (43). Moreover, OCT images of enamel carious lesions predominantly show very low signal intensity from the structure immediately beneath the demineralized lesion, and it may be difficult to detect the location of dentino-enamel junction (DEJ) at these locations (37). Therefore, in the current work the potential of an attenuation parameter for assessment of lesion was investigated. The Beer-Lambert law equation employed in this study is based on a simple and well-established model

assuming only a single back-scattering event during light propagation in the tissue at low optical depths (7, 36). The factor of 2 in the exponent of Eq. (1) corresponds to the double distance of the backscatter light in OCT imaging.

In order to validate the attenuation parameter μ_t, nanoindentation hardness was used to objectively measure an actual physical property of enamel structure. Hardness has for long been accepted as a measure of mineral density of the hard tissue derived from transverse microradiography (44). and nanoindentation at short depth increments, made possible by a precise specimen displacement stage, has shown promising results in characterization of enamel nanostructure at large (21). The outcome of nanohardness testing validated the OCT findings over a wide range of INH values in the current study. The sound enamel showed the smallest μ_t that was proximate to zero, while the DEM revealed the highest value, indicating a strong attenuation through the lesion. In REM area of the test groups, μ_t values consistently decreased. These findings confirmed that remineralization within the lesion decreased the OCT signal attenuation.

Although remineralization had occurred in the test groups, the INH and μ_t were significantly different from those of sound enamel. This could be attributed to the composition of enamel structure; the apatite crystals require a prolonged period to complete re-crystallization in an environment supersaturated with regard to apatite crystals (20). Moreover, mineral aggregation at the superficial zone may result in a decreased rate of mineral deposition at the deeper areas due to blockage of diffusion pathways. Such hampering effect would depend on several factors including the pH and molecular size of the remineralizing compound, surface zone characteristics, pore sizes throughout the lesion and demineralized depth (29). Permeability of the surface layer has an influence on infiltration (45). and may affect remineralization of the

enamel lesion (46). Nevertheless, the top-down remineralization phenomenon of subsurface lesions would still be clinically desirable over the situation where the early enamel lesion progresses towards cavitation or dentin involvement. Under the clinical conditions, mineral deposition over the surface is less likely, due to the presence of calcium phosphate precipitation inhibitors, salivary proteins and plaque, acting as a fine membrane reducing mineral gains at the surface layer, and cyclic fluctuations in the plaque pH (47, 48).

In the current study, the surface layer thickness, which represented the changes from the surface to the subsurface lesion, was around 10 μm in thickness (49). It appeared that the addition of fluoride in the remineralizing solution had improved the outcome by enhancing a rapid remineralization, which was apparent from μ_t results at 4 days. It was previously found that the increased hardness at the superficial zone of enamel lesions remineralize in situ was a result of better crystalline structure and formation of more acid-resistant and denser fluoridated apatite crystal, in the presence of slightly elevated salivary fluoride levels and bioavailable calcium and organic phosphate (21).

Within the limitations of this in vitro study, the first and second hypotheses of this study were rejected. The SS-OCT was able to detect small enamel remineralization changes, and there was a significant correlation between optical and mechanical findings. In order to adopt such an optical parameter for clinical image analysis, it is also important to control the factors that can non-uniformly affect signal patterns and attenuation. Under conventional OCT, the reflection from surface results in a strong signal peak that may interfere with signal analysis (15). It has been shown that hydration state affects the OCT signal intensity from enamel lesions in proportion to the demineralization extent (35). In the current study, imaging was performed under controlled hydrated conditions to minimize the effects of hydration factor and resemble the

humid oral environment. Clinically, blot drying or gentle air drying of the surface would be necessary to remove excessive amount of saliva or water over the area of interest. Also, cleaning the surface before imaging is essential as plaque and calculus could interfere with the light propagation through the lesion. Likewise, a protective cover placed over the OCT intraoral imaging probe for infection control pruposes may refract and attenuate non-uniformly; therefore an autoclavable OCT intraoral probe that requires no disposable cover is desirable. It is also noteworthy that the depth of field is restricted in the current OCT systems; therefore, controlling the object-probe distance is important to maintain the image focused and avoid signal loss. Finally, monitoring of an enamel lesion based on the OCT signal attenuation over time appears to be a promising approach; however, the method should be tested for a larger range of lesions with various shapes, structures and depths in the future studies.

2.5 CONCLUSION

Although POs-Ca+F demonstrated a rapid remineralizing effect, similar outcome were obtained from both remineralizing solutions. Attenuation coefficient calculated from OCT signal revealed its potential in assessment of the early enamel lesions as well as the remineralization process, which can be implemented clinically to monitor lesion mineralization progress.

2.6 ACKNOWLEDGMENT

This work was supported by a grant from Japanese Ministry of education, Global Center of Excellence Program (GCOE), International Research Center for Molecular Science in Tooth and Bone Diseases; the Research Grant for Longevity Sciences (21A-8) from Ministry of Health, Labor, and Welfare; and Grant-in-Aid for Scientific Research (Nos. 23659886 and 24792019) from the Japan Society for the Promotion of Science (JSPS). Authors are also grateful to Drs. Ilnaz Hariri and Sahar Khunkar for their assistance. POs-Ca was donated by Ezaki Glico Company for this research.

CHAPTER 3: CHARACTERIZATION OF TRANSPARENT DENTIN IN ATTRITED TEETH USING OPTICAL COHERENCE TOMOGRAPHY AND NANOINDENTATION

CHAPTER 3

CHARACTERIZATION OF TRANSPARENT DENTIN IN ATTRITED TEETH USING OPTICAL COHERENCE TOMOGRAPHY AND NANOINDENTATION

3.1. INTRODUCTION AND OBJECTIVES

With aging, attrition and wear of enamel and dentin surfaces may occur due to prolonged friction of the opposing teeth, causing loss of enamel outer layer and exposure of the dentin tissue. The underlying dentin beneath worn out enamel will undergo pathological and physiological alterations. This altered substrate has been called transparent or sclerotic dentin in the literature. The formation of this dentin is thought to be a natural protective response to the irritation which includes attrition and partly as a consequence of colonization by the oral micro flora. It has been suggested that the fluid inside dentinal tubules will attract the immunoglobulin from the immune system to defend against this bacterial invasion (50). Simultaneously, there is an increase of mineralization of the surrounding tubules. This results in a constriction of the tubules, which is an attempt to minimize the bacterial progression (51). It has been suggested that the constriction of tubules is due to a continuous inward growth of peritubular dentin which can be microscopically observed on the subsurface of attrited teeth (52). Partial or complete obliteration of the dentinal tubules with the sclerotic cast is commonly characterized by shiny surface with some staining, and dentin can be translucent or transparent due to alteration of the crystal shape and structure inside the tubules (53, 54).

Characterization of transparent dentin of attrited teeth is clinically important, since the bonding of resin composites that are increasingly used to restore the lost tissue may be affected by sclerosis and reduced permeability of the tissue (55-57). In other words, with a larger area of the transparent dentin it is more challenging to achieve a successful adhesion with the resin-based dental bonding. Although a modified system has been used to classify the dentin sclerosis clinically, clinical observation is relatively subjective with low sensitivity (58). It is difficult to estimate the thickness or depth of transparent dentin clinically by visual inspection. While the presence of mineral casts in dentinal tubules may result in increased radio-opacity, a conventional radiographic technique is not recommended in such a case, as minimal changes in superficial dentin cannot be detected in dental X-rays. Moreover, super-imposition may occur with adjacent anatomical structures which lead to false or inaccurate reading.

Recently and with advancement in the optical imaging systems, optical coherence tomography (OCT) has been considered in the literature as a high resolution, non-invasive, cross sectional imaging of the tissue microstructures (7, 59). This technology was established in the early 1990's for ophthalmology applications (60, 61). It was developed based on the concept of low-coherence interferometry; a laser source is projected over a sample, and the backscattered signal intensity from within the scattering medium is coupled with the reference light reflected from a mirror. The interference fringes reveal depth-resolved information about scattering and reflection of the light in the sample. The signal from serial linear scans can be transformed into an image by software (62). OCT technology has significantly advanced in recent years by the development of spectral discrimination techniques, which provide a substantial increase in sensitivity over traditional time-domain OCT (63). Swept-source OCT (SS-OCT) is one of the most recent implements of the spectral discrimination, using a wavelength-tuned near-infrared

laser as the light source and providing improved imaging resolution and scanning speed. In the field of dentistry, this new imaging diagnostic tool has demonstrated its capability in identifying the defects and changes at restoration, enamel and superficial dentin layer (26, 64). The differences in backscatter intensity signal from various dental structures were suggested to be caused by the complexity of the tissue composition and orientation, as well as the contrast between the optical properties of enamel and dentin. In dental lab, it was reported that SS-OCT has the ability to differentiate between carious and sound tissues, estimate the lesion depth in demineralized tissue, observe gaps and defects in dental restorations and detects tooth cracks (11, 25-27, 35). In clinical studies conducted with prototype dental OCT probes, the modality demonstrated a high sensitivity to detect carious lesion (65). Nevertheless, no study has reported on the characterization of non-carious transparent dentin by OCT. The aim of this study is to evaluate the optical changes that occur in the dentin of attrited teeth using SS-OCT and to compare the results with light microscopy images and characterize the mechanical properties by *nanoindentation.* Nanoindentation allows the investigation of selected material properties on small amounts of materials, based on the load–displacement data of indentations on a submicron scale. Measurement of mechanical properties by nanoindentation has been suggested as advantageous over the conventional methods- as knoop hardness test- for its high resolution of force and accurate indent positioning. This method has been used to measure hardness and modulus of elasticity of the tooth structure by some researchers (66).

3.2. MATERIALS AND METHODS

3.2.1 SELECTING OF THE TEETH

The experimental plan of this study and the use of extracted human teeth were subjected to the policy of the Ethics Committee of Tokyo Medical and Dental University. Thirty six, human teeth were used in this study. Twelve non-carious anterior teeth were selected as control group with artificial tooth loss; intact enamel and superficial dentin were removed to have the same criteria for the transparent teeth. Twelve anterior and posterior teeth with attrition and exposed transparent dentin surface for the experimental group. Twelve carious teeth were selected as another group for comparison. These teeth were stored in 0.02% thymol with distilled water in 4℃ for about 3-6 months. Teeth selection with attrition were based upon the following criteria; the surface has glossy and smooth appearance with slight discoloration of the surfaces, most of the teeth have saucer shape attrition, no caries involvement.

3.2.2 OCT SYSTEM

The SS-OCT system (OCT-2000®, Santec, Komaki, Japan) used in this study had the same setup components as described by Shimada *et al* (26). It is a frequency domain OCT system integrating a high-speed frequency swept external cavity laser, of which the probe power is less than 20 mW, within the safety limits defined by American National Standards Institute. The light source in this system sweeps the wavelength from 1260 nm to 1360 nm at 20 kHz sweep rate with central wavelength at 1319 nm. The axial resolution of this OCT system is 11 μm in air which corresponds to approximately 7 μm within a biomedical structure with a refractive index of around 1.5. The lateral resolution of 17 μm is determined by the objective lens at the probe. The focused light-source beam is projected onto the sample and scanned across the area of interest in two dimensions (x, z) using a hand-held probe. Backscattered light from the sample is returned to the system, digitized in time scale and then analyzed in the Fourier domain to reveal the depth-resolved reflectivity profile (A-scan) at each point.

The combination of a series of A-scans along the section of interest creates a raw data file (B-scan) with information on the signal intensity (backscattered light) and x, z coordinates from each point within the scanned area. Two-dimensional cross-sectional images can be created by converting the B-scan raw data into a gray-scale image (Fig.1).

3.2.3 OCT IMAGING OF THE SPECIMENS

The hand-held scanning probe connected to the OCT system was set at 5 cm distance from the specimen surface, with the scanning beam oriented about 90 degree to the surface. A custom-made jig was mounted on a micrometer stage to keep each specimen surface parallel to the probe plane.

All the specimens were removed from the water, cleaned with ultrasonic and washed by distilled water. Before imaging, the roots of the selected teeth were cut away. Then OCT images were scanned in controlled hydrated condition after blot drying of the surface with no visible water droplets (35). Transparent surface was observed at some areas with shiny or translucent dentin and images with SS-OCT were taken mesio-distally at 500 μm interval. About six images were taken for anterior teeth and 10 images for the molars. Many images were taken from different teeth with transparent, carious dentin and sound one for comparison. OCT beam were directed parallel to the dentinal tubules as all the transparent dentin located occlusally.

3.2.4 OCT IMAGE ANALYSIS

For image analysis, a custom code in the image analysis software (ImageJ version 1.47n; Wayne Rasband, NIH, Bethesda, Maryland) was used to read the raw data of the OCT. The obtained OCT image was rotated to compensate for the tilting during scan and reach a horizontal surface. A noise reducing median filter (size 2) was applied to the data. A region of interest (ROI) width

200 μm × optical depth 400 μm from the surface of dentin to deeper levels was selected and converted to signal intensity depth profile.

The OCT-attenuation coefficient (μ_t) was calculated on each average signal intensity profile based on the exponential decay of irradiance from beneath the surface by 20 μm to get rid of the high Fresnel reflection of the surface of the specimen, using the equation derived from Beer-Lambert law, in the following function (36).

$$I(z) = ce^{-2\mu_t z} \quad \text{Eq. (1)}$$

Where I is the reflectivity signal intensity in (dB), c is a constant and z is the depth variable which takes a factor of 2. μ_t was calculated using linear least-squares regression to fit the natural log of average OCT profiles obtained from the ROI.

3.2.5 LIGHT MICROSCOPY

The teeth were cut with a low speed diamond saw (Isomet; Buehler, Lake Bluff, IL, USA) under running water into slices longitudinally (2.5 mm thickness) and two slices were obtained from each specimen. Then, polishing was done with silicon carbide paper starting from 600 grit and up to 2000 grit followed by polishing with diamond films and pastes #6, 3, 1, and ¼ μm respectively. After polishing was done, specimens were ultrasonicated in the machine for 10 minutes to remove any debris from the polished surfaces. Imaging of the specimens was done under light microscope (Nikon SMZ1000 Stereomicroscope), which is a parallel optical zoom system; the lens has intermediate magnification 1.5x with zoom range: 0.8x to 8.0x.

3.2.6 NANOHARDNESS TEST

Mechanical properties evaluation for the transparent dentin was conducted by a nanoindentaion technique (Elionix ENT-1100a, Japan) with a Berkovich indentor, a three sided pyramid tip which can record small load and displacement with high accuracy and precision in the sub micro scale. Specimens were fixed on the stage, 30 points were selected in the transparent zone, 10 points in each raw with 20μm space between each point on the same row and 10μm between each row, then after the 4th row we increase the distance to 50 um, after that, 100 μm a maximum of 150-200 points were obtained in each specimen with a constant force of 10 mN and 1000 milliseconds holding time. To calculate Martens hardness (H) in MPa, the load was divided over the projected area under maximum load which would include both elastic and plastic deformation.

$$H = \frac{Force}{Contact\ area} \quad \text{Eq. (3)}$$

In addition to the hardness profile for each area, nanohardness (NH) values were calculated for the whole area from the surface up to 600 μm depth.

3.2.7 STATISTICAL ANALYSES

Kolmogorov Smirnoff tests were used to determine normal distribution of the data and select proper analyses. Attenuation coefficient values were analyzed by one-way ANOVA with Tukey's post-hoc between the groups. Two-way ANOVA was used to compare the nanohardness of transparent dentin to sound dentin in the first 30 μm and up to 400 μm All

statistical analyses were performed with 95% level of confidence with Statistical Package for Medical Science (SPSS Ver.11 for Windows, SPSS, Chicago, IL, USA) ($\alpha = 0.05$).

3.3 RESULTS

OCT images of sound, carious and transparent dentin are presented in Figures 8 and 9. As the light passed through dentin, SS-OCT was able to detect some changes in superficial layer of transparent dentin. A high intensity with a high backscattered reflection on the 1st 400 μm (optical depth) of the exposed dentin surface was illustrated in the B-scan images and decrease at deeper level. In carious dentin, although there was an increase in the backscattered light in the superficial layer, there was a sharp decrease of signals in the deepest part. Oppositely, the light intensity was average in sound dentin starting as mid-high and gradually decreased (Fig. 7). OCT was able to detect some cracks in the enamel layer in some samples as in Fig. 8(c, e).

The corresponding images of light microscope in Figure 8(b, d, f) showed lack of orientation of dentinal tubules and optical changes in the superficial surfaces of transparent dentin. ImageJ was used for analysis of the raw data, signal intensity profiles were obtained for sound, transparent and carious dentin at 2 mm and at 400 μm depth as shown in Fig.9(a,b). μ_t was calculated from the fitted line of signal intensity profile. The mean values of μ_t were 1.05 ±0.3 mm^{-1}, 2.23 ±0.4 mm^{-1} and 0.61 ±0.27 mm^{-1} for sound, carious and transparent dentin respectively. The μ_t of transparent dentin recorded the lowest value compared to sound and carious dentin, One way ANOVA of different groups showed significantly difference with Tukey's post-hoc ($p<0.05$), as prescribed in Figure 10.

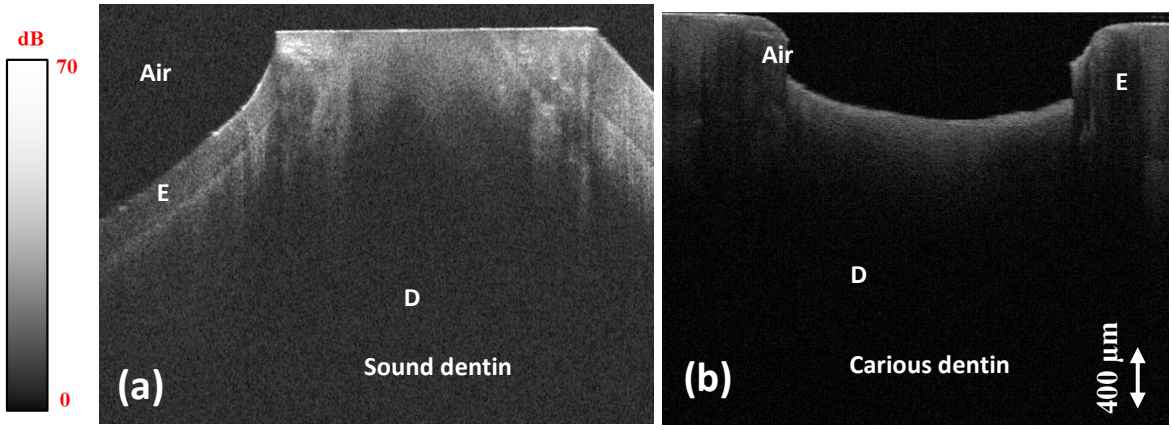

Figure 7:- SS-OCT B-scan images of sound and carious teeth. (a) Incisal enamel of a sound incisor was cut away to expose a similar dentin region as in attrited teeth. (b) Dentin was exposed due to a deep caries lesion with enamel breakdown. OCT signal from the bacteria-infected soft carious dentin appears to be limited in depth.

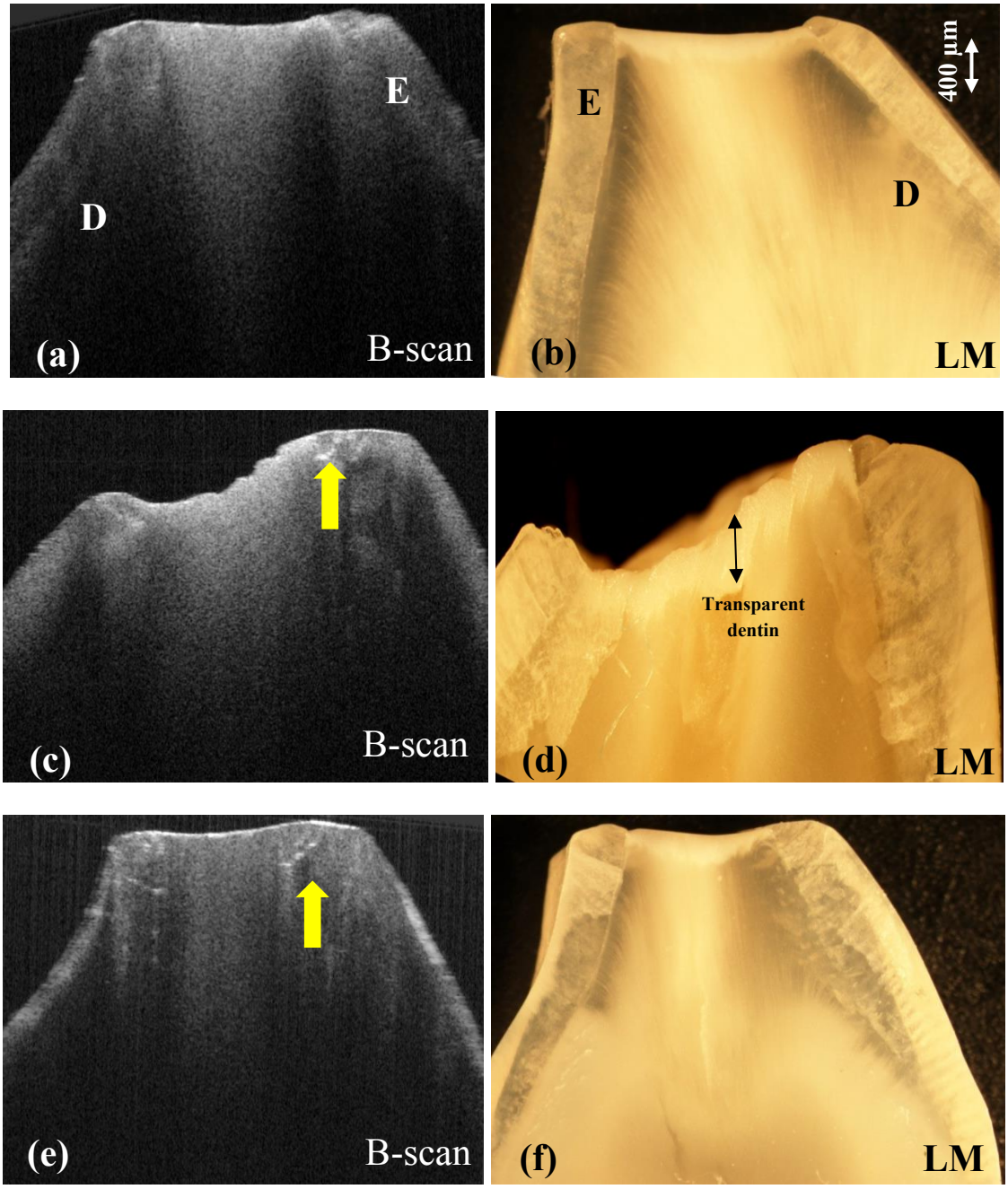

Figure 8- : Images of incisors with attrited incisal edges. (a, c, e) SS-OCT b-scan image shows dentinal changes at the superficial layer as high signal intensity with an increase in the backscattered reflection. (b, d, f) The corresponding images of specimen were examined under visible light microscope and showed a distinct layer of transparent, shiny dentin immediately at the subsurface zone.

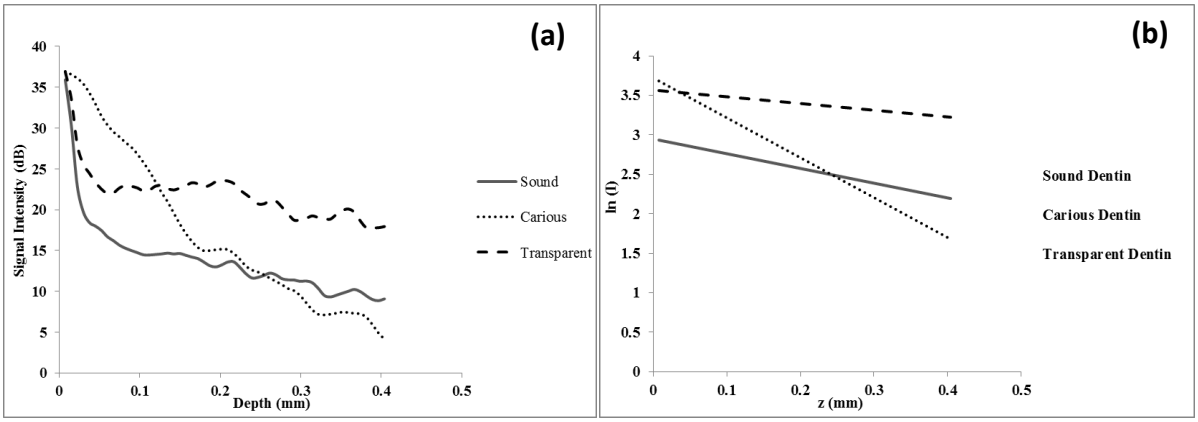

Figure 9- : (a) Signal intensity profile of sound, transparent and carious dentin at 400 µm depth. Transparent dentin shows higher signal levels than carious and sound dentin. (b) An OCT attenuation coefficient (μ_t) was calculated using linear least –squares regression to fit the natural log of average OCT profiles obtained from ROI. The transparent dentin has the lowest μ_t while the carious has the highest.

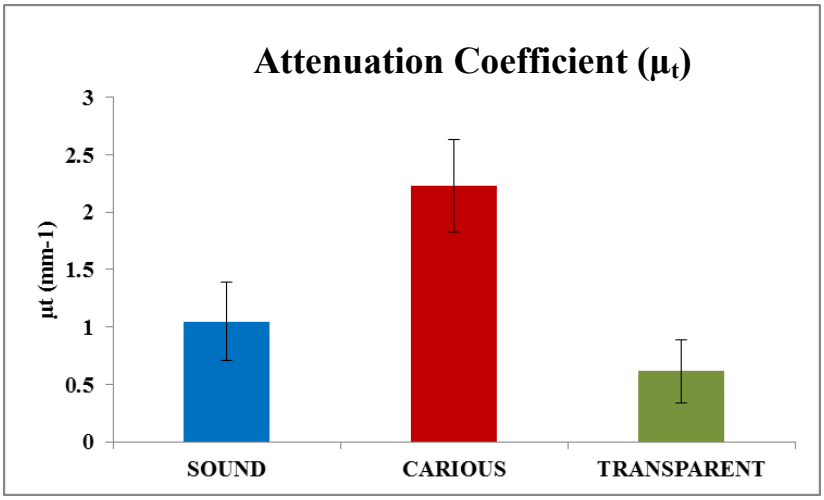

Figure 10- : The bar graph shows average µt of different groups. The 3 groups were significantly different from each other ($p<0.05$).

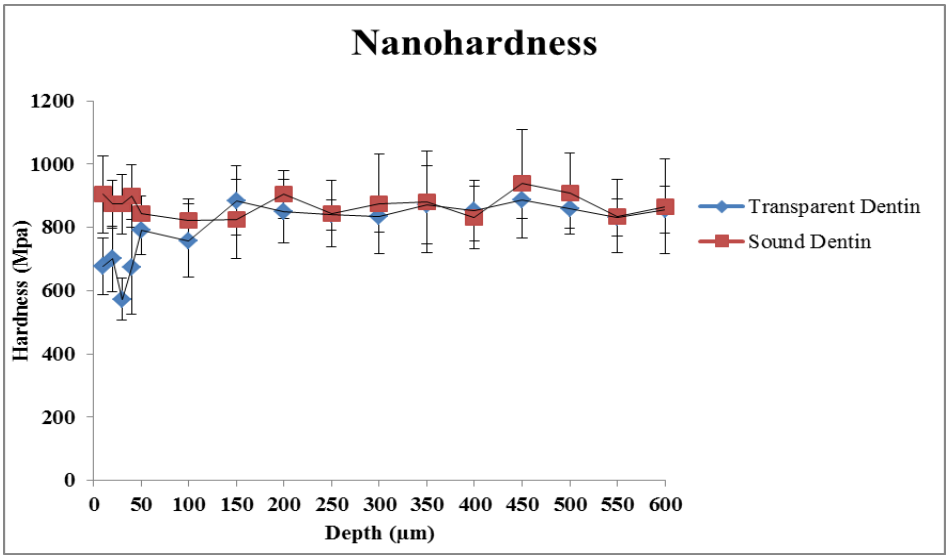

Figure 11- : Testing the mechanical properties of the transparent dentin showed a decrease in the hardness and modulus of elasticity at the superficial layers in comparison to the sound dentin specimen, Two-way ANOVA ($p<0.001$)

Mechanical testing of the transparent dentin revealed reduced hardness and modulus of elasticity in the first 30 µm which is similar to Martins et al study (66). There is an inverse relation between increase the sclerosis and decrease the hardness of dentin. The more sclerosis, the least attenuation the more light transparency became. Two way ANOVA showed that there is significant differences in hardness in the first 30 microns layers ($p<0.001$) shown in Fig.11.

3.4 DISCUSSION

SS-OCT is one of the latest applications of OCT imaging technology that provides cross-sectional images with higher resolution and speed compared to the conventional time-domain systems, permitting instant imaging of the dental hard tissue. It has been reported that the imaging depth of OCT systems is in the range of 2–3 mm, depending on the optical attenuation parameters within the substrate being imaged (26). It has been proven that at 1310 nm, enamel

structure tends to be more transparent than dentin with less scattering in deeper layer (67). Attenuation coefficient of enamel recorded lower value comparing to dentin, this was due to the relatively homogeneous structure of enamel with approximately 87 vol. % of minerals, where presence of inorganic apatite-like crystals are clustered together in the form of prisms. However, attenuation coefficient of dentin is much higher than that of enamel, as the dentin contains over 50 vol. % of organic structure (mainly collagen) and fluid (mainly water), which scatters and absorbs the light. Moreover, the presence of tubules (acting as hollow or water filled defects) and their orientation have a great influence on scattering and attenuation of the light (68).

In a previous study, attenuation coefficient appeared to be a valid parameter in determining between sound, demineralized and remineralized enamel, when other factors such as the tissue moisture and depth of comparison were controlled (69). It was suggested that demineralization of enamel resulted in rapid loss6 of backscatter signal due to the increased porosity of the tissue; light scattering at the boundaries of these micro pores results in the decay of the signal, indicated by a significantly larger attenuation coefficient. While the reflection pattern in dentin is more complicated, the presence of caries in dentin leads to more scattering and consequently higher attenuation coefficient in a similar manner (69, 70). As confirmed by the results of this study, in caries-infected dentin, the signal intensity profile shows different pattern than the sound dentin; loss of signals in the deeper area indicates sever loss of mineral and pathological changes in the superior structure.

On the other hand, the attenuation coefficient μ_t of transparent dentin revealed the lowest values among the dentin substrates. Microscopic assessment of the cross-section suggested that in the samples were the sclerotic changes were more severe a lower μ_t was obtained from OCT signal analysis. This may be attributed to histological changes in dentin that transforms it to a

substrate totally different from the original dentin structure (54, 71). Loss of signal intensity through transparent dentin is lower than those of sound and carious dentin, and on the OCT images deeper scattering can be observed in the center of the occlusal cuspal area. These areas with deep scattering generally corresponded with the transparent dentin area seen on the light microscopy images; nevertheless, it is difficult to define a border for the altered dentin on a histological section. The scattering was extended deeply and was more accentuated in the center of the incisal area of severely attrition zone. This may be due to the presence of sclerotic casts and mineral depositions inside the dentinal tubules that allow light to pass through with minimal loss of intensity. In this regard, the transparent dentin appears to be behaving similar to the highly mineralized enamel tissue in terms of optical transmittance. However, it should be noted that in terms of mechanical properties, the transparent dentin is far weaker than the enamel due to the irregular structure formed by deposition of mineral casts that can be different from apatite-crystals, and the fact that the superficial transparent dentin after loss of enamel has been exposed to environmental challenges such as some bacterial penetration. It has been mentioned in the literature that in high resolution microscope, the intertubular mineral crystallites were smaller in transparent dentin as compared to normal dentin and a plate-like apatite crystallites were present (72). Oppositely, intratubular mineral of transparent dentin deposited larger hydroxyapatite crystals within the tubules in transparent dentin (73).

It is significant to mention that the attenuation of light differs with the orientation of dentinal tubules in the sound dentin due to the complex structure of the tissue, which in return will affect the refractive index of the dentin (74, 75). While imaging the attrited occlusal surfaces, the light is not perpendicular to the original direction of tubules; hence, less variation from dentinal tubule orientations can be expected. Moreover, light microscopy images indicated that

the superficial dentin had an undefined dentinal tubule pattern which differed from sound dentin histologically and optically.

However, mechanical properties of transparent dentin did not change dramatically than sound dentin, although there was accumulation of sclerotic casts inside dentinal tubules. Nanohardness of superficial layer of 30 μm demonstrated decrease in the hardness, this results was somehow similar to previous result of transparent dentin under carious lesion (50). Unlike previous study which has higher hardness of transparent dentin of non-exposed dentin (76).

It is noteworthy to mention that the dentin is supported by enamel, and loss of supporting layer may develop weak dentin layer that is more susceptible to bacterial invasion. Therefore, transparent dentin impedes the development of carious lesion in the form of irregular dentinal tubules that differ optically and histologically from the normal dentinal tubules.

Clinically, intraoral OCT imaging can assist the dental professionals to characterize the tooth substrate in their treatment planning, especially for the complicated wear and elderly cases. Further investigations with other confirmatory tests are needed to endorse the obtained results of this study.

3.5 CONCLUSION

SS-OCT showed its remarkable ability in evaluation of the dentin substrate non-destructively and non-invasively. OCT signal patterns at the 1300 nm region were different between sound, carious and transparent dentin at similar anatomical regions. Transparent dentin exposed on the attrited occlusal surface was characterized by a low OCT attenuation coefficient, due to the deposition of crystallites in the dentinal tubules.

Despite the limitation within this study, nanoindentation had revealed the reduced mechanical properties of the physiologically attrited dentin (transparent dentin).

3.6 ACKNOWLEDGMENT

This work was supported by a grant from Japanese Ministry of education, Global Center of Excellence Program (GCOE), International Research Center for Molecular Science in Tooth and Bone Diseases; the Research Grant for Longevity Sciences (21A-8) from Ministry of Health, Labor, and Welfare; and Grant-in-Aid for Scientific Research (Nos. 23659886 and 24792019) from the Japan Society for the Promotion of Science (JSPS).

CHAPTER 4

CHAPTER 4

GENERAL CONCLUSIONS

In both two studies, experiments were done in the laboratory. However, the potential for OCT-based diagnostics in the oral cavity is excellent. The penetration depth of this modality is adequate for most dental applications.

Based on the data available and the obtained results from the presented studies, a number of factors influencing the OCT signals and the attenuation coefficient.

- In chapter 2, SS-OCT imaging technology demonstrated a remarkable capability with high sensitivity in detection and monitoring small remineralization of enamel subsurface lesion. Although POs-Ca+F demonstrated a rapid remineralizing effect, similar outcome were obtained from both remineralizing solutions. Attenuation coefficient calculated from OCT signal revealed its potential in assessment of the early enamel lesions as well as the remineralization process, which can be implemented clinically to monitor lesion mineralization progress.
- In chapter 3, OCT was able to detect the superficial optical change of transparent dentin in attrited teeth, which demonstrates a lower attenuation coefficient comparing to sound and carious dentin. The obtained results from this study will aid in better understanding of the physiological changes in the tooth structure that accompanied with aging. Clinically, it will assist the dental professionals during their restorative treatment, especially for the elderly patients.

This work will have an important role in the laboratory and clinical monitoring and detecting physiological or pathological changes in dental hard tissue.

Finally, this non-invasive imaging technique has a great potential for improving diagnostic and educational capabilities in oral cavity for applications ranging from early lesions, through periodontal diseases to oral malignancies.

BIBLIOGRAPHY

BIBLIOGRAPHY

1. Tomes CS. On the Chemical Composition of Enamel. *J Physiol* 1896;**19**(3):217-23.

2. White SC, Frey NW. An estimation of somatic hazards to the United States population from dental radiography. *Oral Surg Oral Med Oral Pathol* 1977;**43**(1):152-9.

3. Rechmann P, Rechmann BM, Featherstone JD. Caries detection using light-based diagnostic tools. *Compend Contin Educ Dent* 2012;**33**(8):582-4, 86, 88-93; quiz 94, 96.

4. Rechmann P, Charland D, Rechmann BM, Featherstone JD. Performance of laser fluorescence devices and visual examination for the detection of occlusal caries in permanent molars. *J Biomed Opt* 2012;**17**(3):036006.

5. Pretty IA. Caries detection and diagnosis: novel technologies. *J Dent* 2006;**34**(10):727-39.

6. Mitropoulos P, Rahiotis C, Kakaboura A, Vougiouklakis G. The impact of magnification on occlusal caries diagnosis with implementation of the ICDAS II criteria. *Caries Res* 2012;**46**(1):82-6.

7. Huang D, Swanson EA, Lin CP, Schuman JS, Stinson WG, Chang W, et al. Optical coherence tomography. *Science* 1991;**254**(5035):1178-81.

8. Yamanari M, Lim Y, Makita S, Yasuno Y. Visualization of phase retardation of deep posterior eye by polarization-sensitive swept-source optical coherence tomography with 1-mu m probe. *Optics Express* 2009;**17**(15):12385-96.

9. Bakhsh TA, Sadr A, Shimada Y, Tagami J, Sumi Y. Non-invasive quantification of resin-dentin interfacial gaps using optical coherence tomography: validation against confocal microscopy. *Dent Mater* 2011;**27**(9):915-25.

10. Shimada Y, Sadr A, Burrow MF, Tagami J, Ozawa N, Sumi Y. Validation of swept-source optical coherence tomography (SS-OCT) for the diagnosis of occlusal caries. *J Dent* 2010;**38**(8):655-65.

11. Makishi P, Shimada Y, Sadr A, Tagami J, Sumi Y. Non-destructive 3D imaging of composite restorations using optical coherence tomography: marginal adaptation of self-etch adhesives. *J Dent* 2011;**39**(4):316-25.

12. Le MH, Darling CL, Fried D. Automated analysis of lesion depth and integrated reflectivity in PS-OCT scans of tooth demineralization. *Lasers Surg Med* 2010;**42**(1):62-8.

13. Kang H, Darling CL, Fried D. Nondestructive monitoring of the repair of enamel artificial lesions by an acidic remineralization model using polarization-sensitive optical coherence tomography. *Dent Mater* 2012;**28**(5):488-94.

14. Jones RS, Darling CL, Featherstone JD, Fried D. Remineralization of in vitro dental caries assessed with polarization-sensitive optical coherence tomography. *J Biomed Opt* 2006;**11**(1):014016.

15. Natsume Y, Nakashima S, Sadr A, Shimada Y, Tagami J, Sumi Y. Estimation of lesion progress in artificial root caries by swept source optical coherence tomography in comparison to transverse microradiography. *J Biomed Opt* 2011;**16**(7):071408.

16. Arends J, Christoffersen J. The nature of early caries lesions in enamel. *J Dent Res* 1986;**65**(1):2-11.

17. Larsen MJ, Fejerskov O. Chemical and structural challenges in remineralization of dental enamel lesions. *Scand J Dent Res* 1989;**97**(4):285-96.

18. Torres MG, Santos AaS, Neves FS, Arriaga ML, Campos PS, Crusoé-Rebello I. Assessment of enamel-dentin caries lesions detection using bitewing PSP digital images. *J Appl Oral Sci* 2011;**19**(5):462-8.

19. Schemehorn BR, Orban JC, Wood GD, Fischer GM, Winston AE. Remineralization by fluoride enhanced with calcium and phosphate ingredients. *J Clin Dent* 1999;**10**(1 Spec No):13-6.

20. Kitasako Y, Tanaka M, Sadr A, Hamba H, Ikeda M, Tagami J. Effects of a chewing gum containing phosphoryl oligosaccharides of calcium (POs-Ca) and fluoride on remineralization and crystallization of enamel subsurface lesions in situ. *J Dent* 2011;**39**(11):771-9.

21. Kitasako Y, Sadr A, Hamba H, Ikeda M, Tagami J. Gum Containing Calcium Fluoride Reinforces Enamel Subsurface Lesions in situ. *J Dent Res* 2012;**91**(4):370-5.

22. Jablonski-Momeni A, Stachniss V, Ricketts DN, Heinzel-Gutenbrunner M, Pieper K. Reproducibility and accuracy of the ICDAS-II for detection of occlusal caries in vitro. *Caries Res* 2008;**42**(2):79-87.

23. Haak R, Wicht MJ, Noack MJ. Conventional, digital and contrast-enhanced bitewing radiographs in the decision to restore approximal carious lesions. *Caries Res* 2001;**35**(3):193-9.

24. Karlsson L. Caries Detection Methods Based on Changes in Optical Properties between Healthy and Carious Tissue. *Int J Dent* 2010;**2010**:270729.

25. Bakhsh TA, Sadr A, Shimada Y, Tagami J, Sumi Y. Non-invasive quantification of resin-dentin interfacial gaps using optical coherence tomography: validation against confocal microscopy. *Dent Mater* 2011;**27**(9):915-25.

26. Shimada Y, Sadr A, Burrow MF, Tagami J, Ozawa N, Sumi Y. Validation of swept-source optical coherence tomography (SS-OCT) for the diagnosis of occlusal caries. *J Dent* 2010;**38**(8):655-65.

27. Imai K, Shimada Y, Sadr A, Sumi Y, Tagami J. Noninvasive Cross-sectional Visualization of Enamel Cracks by Optical Coherence Tomography In Vitro. *J Endod* 2012;**38**(9):1269-74.

28. Le MH, Darling CL, Fried D. Automated analysis of lesion depth and integrated reflectivity in PS-OCT scans of tooth demineralization. *Lasers Surg Med* 2010;**42**(1):62-8.

29. Kang H, Darling CL, Fried D. Nondestructive monitoring of the repair of enamel artificial lesions by an acidic remineralization model using polarization-sensitive optical coherence tomography. *Dent Mater* 2012;**28**(5):488-94.

30. Scolaro L, McLaughlin RA, Klyen BR, Wood BA, Robbins PD, Saunders CM, et al. Parametric imaging of the local attenuation coefficient in human axillary lymph nodes assessed using optical coherence tomography. *Biomed Opt Express* 2012;**3**(2):366-79.

31. van der Meer FJ, Faber DJ, Baraznji Sassoon DM, Aalders MC, Pasterkamp G, van Leeuwen TG. Localized measurement of optical attenuation coefficients of atherosclerotic plaque constituents by quantitative optical coherence tomography. *IEEE Trans Med Imaging* 2005;**24**(10):1369-76.

32. Popescu DP, Sowa MG, Hewko MD, Choo-Smith LP. Assessment of early demineralization in teeth using the signal attenuation in optical coherence tomography images. *J Biomed Opt* 2008;**13**(5):054053.

33. Sadr A, Mandurah M, Nakashima S, Shimada Y, Kitasako Y, Tagami J, et al. Monitoring of enamel lesion remineralization by optical coherence tomography: an alternative approach towards signal analysis. 2013; 2013. p. 856602-02-8.

34. ten Cate JM, Dundon KA, Vernon PG, Damato FA, Huntington E, Exterkate RA, et al. Preparation and measurement of artificial enamel lesions, a four-laboratory ring test. *Caries Res* 1996;**30**(6):400-7.

35. Nazari A, Sadr A, Campillo-Funollet M, Nakashima S, Shimada Y, Tagami J, et al. Effect of hydration on assessment of early enamel lesion using swept-source optical coherence tomography. *J Biophotonics* 2012.

36. Schmitt JM, Knüttel A, Yadlowsky M, Eckhaus MA. Optical-coherence tomography of a dense tissue: statistics of attenuation and backscattering. *Phys Med Biol* 1994;**39**(10):1705-20.

37. Nakagawa H, Sadr A, Shimada Y, Tagami J, Sumi Y. Validation of swept source optical coherence tomography (SS-OCT) for the diagnosis of smooth surface caries in vitro. *J Dent* 2012.

38. Kang H, Jiao JJ, Lee C, Le MH, Darling CL, Fried D. Nondestructive Assessment of Early Tooth Demineralization Using Cross-Polarization Optical Coherence Tomography. *IEEE J Sel Top Quantum Electron* 2010;**16**(4):870-76.

39. Sowa MG, Popescu DP, Friesen JR, Hewko MD, Choo-Smith LP. A comparison of methods using optical coherence tomography to detect demineralized regions in teeth. *J Biophotonics* 2011;**4**(11-12):814-23.

40. Jones R, Huynh G, Jones G, Fried D. Near-infrared transillumination at 1310-nm for the imaging of early dental decay. *Opt Express* 2003;**11**(18):2259-65.

41. Fried D, Featherstone JD, Darling CL, Jones RS, Ngaotheppitak P, Buhler CM. Early caries imaging and monitoring with near-infrared light. *Dent Clin North Am* 2005;**49**(4):771-93, vi.

42. Hariri I, Sadr A, Shimada Y, Tagami J, Sumi Y. Effects of structural orientation of enamel and dentine on light attenuation and local refractive index: An optical coherence tomography study. *J Dent* 2012;**40**(5):387-96.

43. Fried D, Glena RE, Featherstone JD, Seka W. Nature of light scattering in dental enamel and dentin at visible and near-infrared wavelengths. *Appl Opt* 1995;**34**(7):1278-85.

44. Featherstone JD, ten Cate JM, Shariati M, Arends J. Comparison of artificial caries-like lesions by quantitative microradiography and microhardness profiles. *Caries Res* 1983;**17**(5):385-91.

45. Meyer-Lueckel H, Paris S, Kielbassa AM. Surface layer erosion of natural caries lesions with phosphoric and hydrochloric acid gels in preparation for resin infiltration. *Caries Res* 2007;**41**(3):223-30.

46. Cochrane NJ, Cai F, Huq NL, Burrow MF, Reynolds EC. New approaches to enhanced remineralization of tooth enamel. *J Dent Res* 2010;**89**(11):1187-97.

47. Fujikawa H, Matsuyama K, Uchiyama A, Nakashima S, Ujiie T. Influence of salivary macromolecules and fluoride on enamel lesion remineralization in vitro. *Caries Res* 2008;**42**(1):37-45.

48. Bennick A. Salivary proline-rich proteins. *Mol Cell Biochem* 1982;**45**(2):83-99.

49. Groeneveld A, Arends J. Influence of pH and demineralization time on mineral content, thickness of surface layer and depth of artifical caries lesions. *Caries Res* 1975;**9**(1):36-44.

50. Ogawa K, Yamashita Y, Ichijo T, Fusayama T. The ultrastructure and hardness of the transparent layer of human carious dentin. *J Dent Res* 1983;**62**(1):7-10.

51. Tronstad L, Langeland K. Histochemical observations on human dentin exposed by attrition. *Scand J Dent Res* 1971;**79**(3):151-9.

52. Senawongse P, Otsuki M, Tagami J, Mjör IA. Morphological characterization and permeability of attrited human dentine. *Arch Oral Biol* 2008;**53**(1):14-9.

53. Brännström M, Garberoglio R. Occlusion of dentinal tubules under superficial attrited dentine. *Swed Dent J* 1980;**4**(3):87-91.

54. Vasiliadis L, Darling AI, Levers BG. The histology of sclerotic human root dentine. *Arch Oral Biol* 1983;**28**(8):693-700.

55. Tay FR, Pashley DH. Resin bonding to cervical sclerotic dentin: a review. *J Dent* 2004;**32**(3):173-96.

56. Kusunoki M, Itoh K, Hisamitsu H, Wakumoto S. The efficacy of dentine adhesive to sclerotic dentine. *J Dent* 2002;**30**(2-3):91-7.

57. Marshall GW, Marshall SJ, Kinney JH, Balooch M. The dentin substrate: structure and properties related to bonding. *J Dent* 1997;**25**(6):441-58.

58. Ritter AV, Heymann HO, Swift EJ, Sturdevant JR, Wilder AD. Clinical evaluation of an all-in-one adhesive in non-carious cervical lesions with different degrees of dentin sclerosis. *Oper Dent* 2008;**33**(4):370-8.

59. Wang XJ, Milner TE, de Boer JF, Zhang Y, Pashley DH, Nelson JS. Characterization of dentin and enamel by use of optical coherence tomography. *Appl Opt* 1999;**38**(10):2092-6.

60. Izatt JA, Hee MR, Swanson EA, Lin CP, Huang D, Schuman JS, et al. Micrometer-scale resolution imaging of the anterior eye in vivo with optical coherence tomography. *Arch Ophthalmol* 1994;**112**(12):1584-9.

61. Hee MR, Izatt JA, Swanson EA, Huang D, Schuman JS, Lin CP, et al. Optical coherence tomography of the human retina. *Arch Ophthalmol* 1995;**113**(3):325-32.

62. Huang D, Swanson EA, Lin CP, Schuman JS, Stinson WG, Chang W, et al. Optical coherence tomography. *Science* 1991;**254**(5035):1178-81.

63. Choma M, Sarunic M, Yang C, Izatt J. Sensitivity advantage of swept source and Fourier domain optical coherence tomography. *Opt Express* 2003;**11**(18):2183-9.

64. Natsume Y, Nakashima S, Sadr A, Shimada Y, Tagami J, Sumi Y. Estimation of lesion progress in artificial root caries by swept source optical coherence tomography in comparison to transverse microradiography. *J Biomed Opt* 2011;**16**(7):071408.

65. Shimada Y, Nakagawa H, Sadr A, Wada I, Nakajima M, Nikaido T, et al. Noninvasive cross-sectional imaging of proximal caries using swept-source optical coherence tomography (SS-OCT) <?tf="HLBI">in vivo. *J Biophotonics* 2013.

66. Martín N, García A, Vera V, Garrido MA, Rodríguez J. Mechanical characterization of sclerotic occlusal dentin by nanoindentation and nanoscratch. *Am J Dent* 2010;**23**(2):108-12.

67. Fried D, Glena RE, Featherstone JD, Seka W. Nature of light scattering in dental enamel and dentin at visible and near-infrared wavelengths. *Appl Opt* 1995;**34**(7):1278-85.

68. Zijp JR, Bosch JJ. Theoretical model for the scattering of light by dentin and comparison with measurements. *Appl Opt* 1993;**32**(4):411-5.

69. Mandurah MM, Sadr A, Shimada Y, Kitasako Y, Nakashima S, Bakhsh TA, et al. Monitoring remineralization of enamel subsurface lesions by optical coherence tomography. *J Biomed Opt* 2013;**18**(4):46006.

70. Darling CL, Huynh GD, Fried D. Light scattering properties of natural and artificially demineralized dental enamel at 1310 nm. *J Biomed Opt* 2006;**11**(3):34023.

71. Micheletti Cremasco M. Dental histology: study of aging processes in root dentine. *Boll Soc Ital Biol Sper* 1998;**74**(3-4):19-28.

72. Porter AE, Nalla RK, Minor A, Jinschek JR, Kisielowski C, Radmilovic V, et al. A transmission electron microscopy study of mineralization in age-induced transparent dentin. *Biomaterials* 2005;**26**(36):7650-60.

73. Kinney JH, Nalla RK, Pople JA, Breunig TM, Ritchie RO. Age-related transparent root dentin: mineral concentration, crystallite size, and mechanical properties. *Biomaterials* 2005;**26**(16):3363-76.

74. Hariri I, Sadr A, Shimada Y, Tagami J, Sumi Y. Effects of structural orientation of enamel and dentine on light attenuation and local refractive index: An optical coherence tomography study. *J Dent* 2012;**40**(5):387-96.

75. Hariri I, Sadr A, Nakashima S, Shimada Y, Tagami J, Sumi Y. Estimation of the Enamel and Dentin Mineral Content from the Refractive Index. *Caries Res* 2012;**47**(1):18-26.

76. Senawongse P, Otsuki M, Tagami J, Mjör I. Age-related changes in hardness and modulus of elasticity of dentine. *Arch Oral Biol* 2006;**51**(6):457-63.

BIOGRAPHY

Mona M. Mandurah, BDS

Tokyo medical and Dental University

Department of Restorative Science

Cariology and Operative Dentistry

Bunkyo-ku, Yushima 1-5-45

Tokyo 113-5849

Tel: +81-3-5803-5483

Fax: +81-3-5803-0195

E-mail: mona.mandurah@gmail.com

EDUCATION

1999~2005 BDS,King Abdulaziz University (KAU), Jeddah, Saudi Arabia (SA).

2010~2014 PhD Candidate, Cariology and Operative Dentistry, Tokyo Medical and Dental University (TMDU), Japan.

PROFFISSIONAL EXPERIENCE

2005~2006 Internship, KAU hospital, Jeddah, SA.

2006~2010 General Dentist, Ministry of Health, Makkah, SA.

2012~2014 Operative Dentistry, TMDU hospital, Japan.

RESEARCH INTEREST

- Lasers in Dentistry.
- Nanotechnology in dental science.

- Remineralization of dental hard tissue.
- Optical and mechanical characterization of dental hard tissue.

PROFESSIONAL MEMBERSHIP

- Member of International Association of Dental Research (IADR).
- Member of International Association of Dental Research, Japanese division (JADR).
- Member of Global Center of Excellence (GCOE).
- Member of Academy of Operative Dentistry (AOD).
- Member of Optical Society of America (OSA).

CONFERENCES

- **Mandurah MM**, Sadr A, Shimada Y, Tagami J, Sumi Y. Optical and Mechanical characterization of Sclerotic dentin in attrited teeth using Optical Coherence Tomography and Nanoindentation, 134th Meeting of the Japanese Society for Conservative Dentistry (JSCD), Maihama, Japan, June 2011

- Sadr A, **Mandurah M,** Tagami J. Mechanical characterization of two flowable resin composites used as base in a deep cavity by nanoindentation. 134th Meeting of the Japanese Society for Conservative Dentistry (JSCD), Chiba, Japan, June 2011

- **Mandurah MM**, Sadr A, Kitasako Y, Nakashima S, Bakhsh TA, Shimada Y, Tagami J, Sumi Y. Remineralization of Enamel Subsurface Lesion by POs-Ca and POs-Ca+F: Evaluation by Nanoindentation and SS-OCT, 136th Meeting of the Japanese Society for Conservative Dentistry (JSCD), Okinawa, Japan, June 2012

- Sadr A, **Mandurah M,** Nakashima S, Shimada Y , Kitasako Y, Tagami J.
  Monitoring of enamel lesion remineralization by optical coherence tomography: an alternative approach towards signal analysis, Lasers in Dentistry XIX
  San Francisco, California, USA, February 2013

- **Mandurah MM**, Sadr A, Nakashima S, Bakhsh TA, Shimada Y, Tagami J, Sumi Y. Enamel Lesion Remineralization Evaluated by Nanoindentation and Optical Coherence Tomography, IADR general session , Seattle , USA, March 2013

- Bakhsh TA, Sadr A, Shimada Y, **Mandurah MM,** Alsayed EZ, Tagami J, Sumi Y. Non-destructive Evaluation of Internal Cavity Adaptation in Class-II resin Composite, IADR general session , Seattle , USA, March 2013

PUBLICATIONS

1. **Mandurah MM,** Sadr A, Shimada Y, Kitasako Y, Nakashima S, Bakhsh TA, Tagami J, Sumi Y. " Monitoring remineralization of enamel subsurface lesion by optical coherence tomography" J. Biomed. Opt. 18(4) 2013

2. Bakhsh TA, Sadr A, Shimada Y, **Mandurah MM**, Hariri I, Alsayed EZ, Tagami J, Sumi Y. "Concurrent evaluation of composite internal adaptation and bond strength in a class-I cavity" J Dent. 2013 Jan;41(1):60-70

3. Alireza Sadr, **Mona Mandurah**, Syozi Nakashima, Yasushi Shimada, Yuichi Kitasako, Junji Tagami, Yasunori Sumi. "Monitoring of enamel lesion remineralization by optical coherence tomography: an alternative approach towards signal analysis" Proc. SPIE 8566, Lasers in Dentistry XIX, 856602 March 25, 2013